Growth and Characterization of Novel Optoelectronic Materials Based on II-VI Inorganic/Organic Heterostructures

Wisanu Pecharapa*, Anusit Keawprajak, Nawapun Kayunkid, Sakon Rahong, Witoon Yindeesuk and Jiti Nukeaw

Department of Applied Physics, Faculty of Science, King Mongkut's Institute of Technology Ladkrabang, Bangkok 10520, Thailand.

* Corresponding author, E-mail: Kpewisan@kmitl.ac.th

ABSTRACT: Novel optoelectronic materials based on II-VI inorganic/organic low-dimensional heterostructure were successfully grown by electron beam evaporator. The structures were based on ZnSe, tris(8-hydroxyquinoline) aluminum (Alq_3) and N,N'–bis(3-methylphenyl)-N,N'–diphenyl-benzidine (TPD). The surface morphology of the structures was investigated by atomic force microscopy and field emission scanning electron microscope. The optical and electronic properties were examined by photoluminescence, photocurrent and electroreflectance spectroscopy. Photoluminescence spectra of the $ZnSe/Alq_3/ZnSe$ structure attributed to the change of exciton energy as a result of quantum confinement showed the formation of single quantum well structure. The luminescence color can be varied by changing the thickness of the Alq_3 layer. The other heterostructure of $ZnSe/Alq_3/TPD$ was grown on silicon substrate. The wavelength response of this structure shown by photocurrent signal ranged from 450 nm to 1100 nm. Electroreflectance features due to optical transition energy of the single quantum well of this structure were also observed. Under applied voltage, electroreflectance signals showed significant shift due to the quantum confined Stark effect.

KEYWORDS: Inorganic/organic heterostructure, quantum well, ZnSe, Alq_3, TPD.

INTRODUCTION

Recently, thin film devices based on organic materials have gained great attention due to their suitable properties for optoelectronic applications. The remarkable advantages of organic materials include color tunability, low power consumption, and ease of fabrication[1,2]. The most promising applications of organic materials include organic light emitting diodes [3,4], flat panel displayed[5], photodetectors[6] and photovoltaic cells[7]. However, in contrast to inorganic semiconductors, organic semiconductors still have major drawbacks such as slow mobility of carriers and strong chemical interaction between two compounds, which prevents the injection of charges into organic materials[8]. Several methods have been proposed to improve the efficiency of the organic-based devices. The use of hybrid organic-inorganic structures combined with the comparatively good transport properties of semiconductors is one of potential techniques. If an organic material having a broad absorption band in an optical range is located near the inorganic semiconductor, the resonant dipole-dipole interaction between two substances will result in the non-radiative transfer of the semiconductor

excitation energy to the organic substrate[9]. This effect will yield more intense luminescence. Because of large enhancement of the interaction between the organic and inorganic layers, it is also believed that novel functionality combined with properties of the organic and inorganic layers, especially in the form of low-dimensional systems, is expected to appear[10]. For example, thermal evaporation of amorphous multilayer of copper phthalocyanine (CuPc) and TiO_2, with a periodicity of 5 nm, forms a composite material with a modulated electronic structure analogous to that of type - II quantum well structures[11,12]. The physical properties of the organic and inorganic quantum well structure are two-dimensional quantum confinement effect due to the large differences in the band gaps and the dielectric constants between layers. The multiple-quantum-well structures of TPD/GaN as organic/inorganic semiconductors have been investigated to ultraviolet-emitting devices[13]. A peak emission wavelength of 400 nm was measured. The external quantum efficiency was about 0.35%.

Photoluminescence (PL) spectroscopy has been extensively used as a characterization tool for fundamental research, especially on low dimensional

systems. PL was employed to investigate the multiple quantum well structures of Alq_3 and 2-(4-biphenylyl)-5(4-tert-butyl-phenyl)-1,3,4-oxadiazole (PBD) prepared by a multisource-type high vacuum organic molecular beam deposition[14]. PL measurement results indicated that the structures had a very uniform layered structure throughout the entire stack. Exciton energy shift to a high energy region with decreasing Alq_3 layer thickness was observed. Modulation spectroscopy is a crucial technique to study and characterize the energy-band structures of semiconductors. Modulation techniques such as electroreflectance (ER) and photoreflectance (PR) spectroscopy are particularly useful since they yield spectra with sharp features at the critical-point energies. The features in the spectra appear at energies corresponding to the band gap characteristic points or other peculiarities in the dielectric function. ER spectroscopy is of considerable interest because it is sensitive to surface and interface electric fields[15,16]. The ER technique was used to study the creation of space charge distributions in a polymer light emitting diode, by monitoring the real third order nonlinear optical response of the electroluminescent layer[17]. The measured signal is strongly influenced by a space charge distribution and by screening in the organic layer. Photocurrent (PC) spectroscopy is also a potential tool to investigate both optical and electronic properties of heterostructure and low-dimensional semiconductor structures. PC technique has the advantage of being a direct measurement in the sense that the current is proportional to the absorption, avoiding huge background, and can be operated at room temperature.

In this work, we report the growth of organic/inorganic heterojunction device. The heterostructures include $ZnSe/Alq_3/ZnSe$ structure on glass substrate and $ZnSe/Alq_3/TPD$ on Si substrate. The chemical structure of organic semiconductors: Alq_3 and TPD, are shown in Fig. 1. The optical and electronic properties of these structures were extensively investigated by PL, PC, and ER spectroscopy. We observed strong visible luminescence from the $ZnSe/Alq_3/ZnSe$ structure. The luminescence color can be varied by changing the Alq_3 layer from 5-50 nm. The wide wavelength response from visible to infrared was observed from the $ZnSe/Alq_3/TPD$ structure. The influence of each compound on optical and electronic properties was discussed. The significant quantum confinement was also observed from both structures.

MATERIALS AND METHODS

We prepared two kinds of structures: $ZnSe/Alq_3/ZnSe$ (structure A), and $ZnSe/Alq_3/TPD$ (structure B). Both structures were prepared using a high vacuum
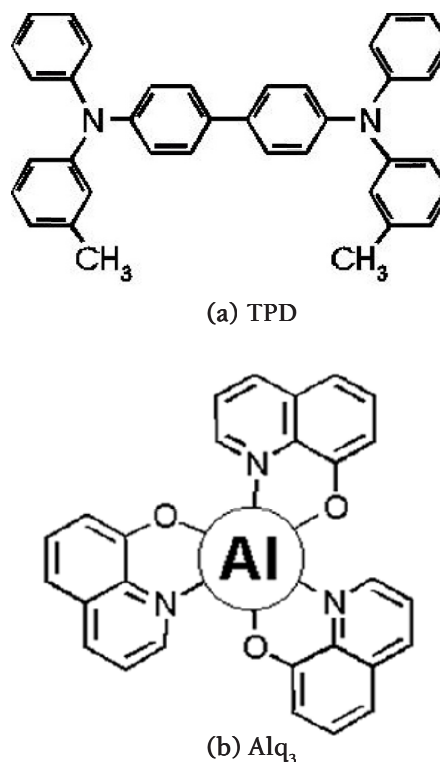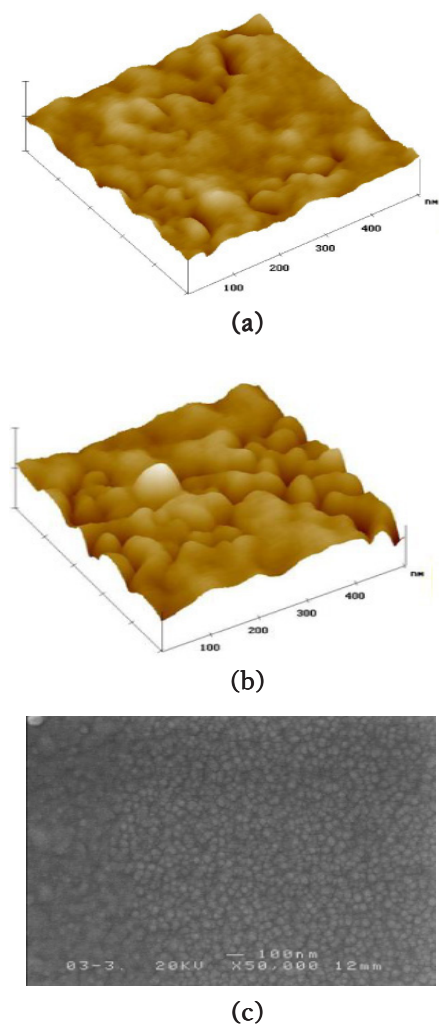

Fig 1. Chemical Structure of (a) TPD, (b) Alq_3.

multi-pocket electron-beam evaporator (Edwards AUTO306) with the base pressure of about 5×10^{-6} mbar. The deposition rate and thickness were measured by a quartz crystal thickness monitor. For structure A, glass plates (superfrost) were used as substrate. Prior to loading into the evaporation chamber, the glass substrate was cleaned in ultrasonic bath successively using deionized water for 15 min, acetone for 15 min, methanol for 15 min and iso-propanol for 15 min. The layer structure was grown starting with a 200 nm ZnSe buffer layer, followed by a Alq_3 emitting layer of various thickness ranging from 10-50 nm, and a 200 nm ZnSe cap layer, respectively. For structure B, the Si substrate was cleaned by Piranha process. The growth process started with a TPD buffer layer of various thickness on Si substrate, followed by Alq_3 layers of various thickness, a 200 nm ZnSe cap layer, and a 200 nm ITO as a transparent front electrode, respectively. The substrate temperature was kept at room temperature for both structures. The surface morphology of the Alq_3 layer without ZnSe cap layer was observed by means of atomic force microscopy (AFM).

A conventional PL experiment was conducted at room temperature (300 K) and at low temperature. An ultraviolet lamp was used as the optical excitation source. The sample was cooled down to 10 K in a cryostat. The luminescence from the sample was

dispersed by a monochromator. The PL signal was amplified by a lock-in amplifier. A computer was used to control the monochromator, collect data from the lock-in amplifier, and produce plots and data files. In ER measurements, DC voltage and AC voltage with frequency of 300 Hz and amplitude of 0.05 V were applied to modulate surface potential. A 100 W tungsten lamp was dispersed by a 25-cm monochromator and used as an excitation source. VIS-Si detector detected the modulation reflectance signal, and the signal from the detector was fed to a lock-in amplifier. For PC spectroscopy, excitation light from tungsten lamp was dispersed by a monochromator. The chopped light was focused on the sample. The PC signal generated, and was detected using a typical lock-in amplifier. All ER and PC measurements were carried out at 300 K.
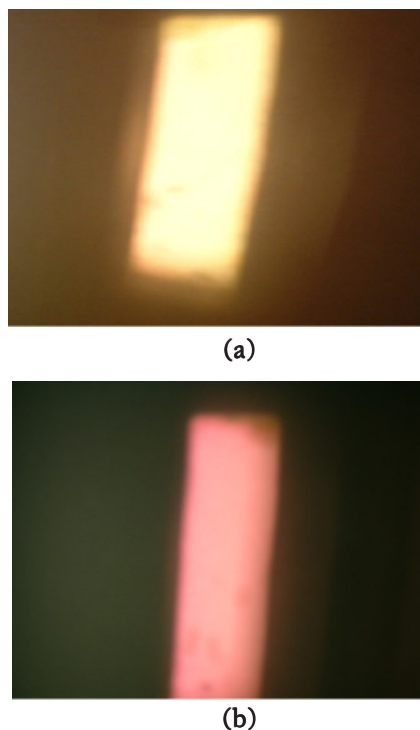
RESULTS AND DISCUSSION

Surface Morphology

Fig. 2 (a) and (b) show AFM images of surface morphology and the roughness of as-deposited Alq_3 thin films with different thickness. The scan size of each AFM image was 500 nm × 500 nm. The AFM images showed that Alq_3 films were in molecular cluster form. The lateral mode images that the surface roughness of Alq_3 thin films increase with increasing thickness. The surface morphologies and roughness of Alq_3 grown by different techniques were investigated[18]. The experiments showed that different growth techniques led to differences in morphology and roughness. In our experiment, Alq_3 thin film was deposited on the substrate only with thermal energy. The thicker film required longer evaporation time than the thinner one. However, without additional kinetic energy, the uniform clusters could not be formed. Therefore, the roughness of the film increased with increasing thickness. The surface morphology of ZnSe film was also investigated by a field emission scanning electron microscope, as seen in Fig. 2(c). The image showed good uniformity of the ZnSe film as nanocrystal with the average size of about 30 nm. It suggested that nanocrystal ZnSe could be grown onto the Alq_3 thin

(a)

(b)

(c)

Fig 2. (a) AFM images of surface morphology of Alq_3 thin films with thickness of 15nm; (b) with thickness of 50 nm; (c) SEM image of ZnSe layer.

(a)

(b)

Fig 3. Room temperature-Luminescence color from structure A with: (a) 20-nm thick Alq_3 layer; (b) 50-nm thick Alq_3 layer.

film by electron beam evaporator.

Photoluminescence

Photoluminescence measurements were conducted on structure A at room temperature. Fig. 3 showed photographs of luminescence from this structure under white light illumination. Intense PL of the sample with Alq_3 layer thickness of 20 nm and 50 nm could be observed by the naked eye in orange and red colors, respectively, suggesting that Alq_3 thickness caused the change in luminescence color. This result suggested that a novel color-tunable organic emitting device based on inorganic/organic heterostructures could be achieved by this technique. Taking the vacuum energy level as a reference, the electronic structure of the conduction band and valence bands of ZnSe were at –4.1 and –6.8 eV below the vacuum level[19], respectively. Meanwhile, the lowest unoccupied molecular orbital (LUMO) and highest occupied molecular orbital (HOMO) levels of Alq_3 were at –4.8 and –6.4 eV, respectively[20]. Based on this fact, the Alq_3 layer acted as a quantum well layer sandwiched between ZnSe potential barriers, and this structure formed a type-I single quantum well, with electrons and holes all confined in Alq_3 layer. The electron and hole potential barriers, i.e. the band offsets, were 0.8 and 0.3 eV, respectively.

Fig. 4 (a) illustrates the PL results of structure A with a well width in a range of 5 to 50 nm at room temperature. There were two distinct broad bands, one at 1.7 eV (λ = 730 nm), and the other at about 2.1 eV (590 nm). Both spectra suggested that this emission should take place in the organic layer because the emission from the ZnSe layer with energy of 2.7 eV was not observed. In addition, the broad luminescence of this structure resulted from inhomogeneous broadening transition mechanism in the organic material. For the sample with the 5 nm Alq_3 layer, two peaks were located at 1.67 eV and 2.05 eV. The higher intensity band at about 1.67 eV was assigned to the radiative decay of triplet states in Alq_3. Meanwhile, the other peak should relate to the recombination of confined excitons in the quantum well. The signal of the higher energy was weak due to the low density of the confined excitons in the quantum well, compared with the density of vibronic progressions. As the quantum well width increased from 5 to 50 nm, the higher energy band exhibited the red shift, moving to lower energy. The shift of the PL peak with increasing quantum well width was attributed to the change of exciton binding energy due to quantum confinement of excitons in two-dimensional layer[22]. The dependencies of the energies of the higher energy PL peaks on the Alq_3 quantum well thickness were shown by the data points in Fig. 4(b). In addition, as the quantum well width increased from 10 to 50 nm, the PL intensity of lower

(a)

(b)
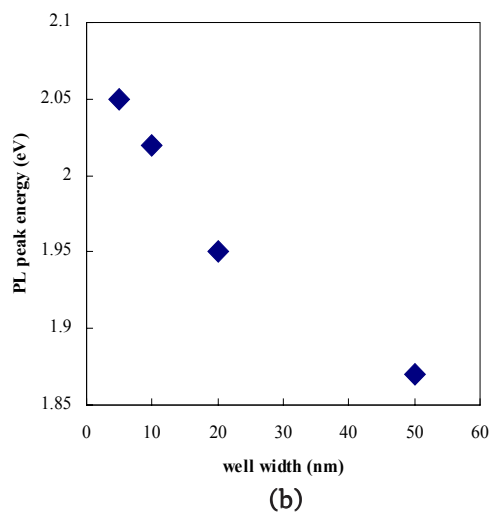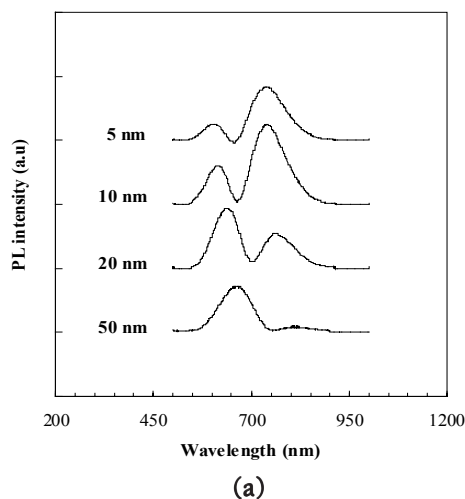
Fig 4. (a) Room temperature-PL of structure A with different well thickness as function of photon energy. (b) Room temperature-PL peak photon energy of structure A as a function of well thickness.

energy band rapidly decreased, but the intensity of the higher energy band became stronger and dominated. These features suggested that the photoinduced exciton density tended to increase as the well width increased.

Fig. 5 showed temperature-dependent PL results of structure A with a well width of 10 nm. When temperature decreased from room temperature to 100 K, the PL intensity increased drastically. The lifetime of the band at 1.7 eV and at about 2.0 eV of Alq_3 was measured by M. Cölle and C. Gärditz[21]. They found that, with decreasing temperature, the lifetime of both bands increased due to reduced phonon–assisted decay of this state. In addition, the experiment showed that the lifetime of the band at 1.7 eV was always greater than the lifetime of the band at about 2.0 eV by a factor of 2. Therefore the concentration of the lower state, i.e. triplet state, was greater than that of the higher state,
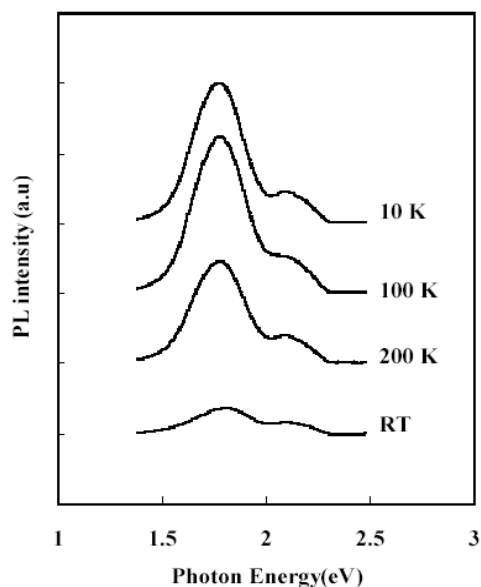
**Fig 5.** Temperature dependent PL of structure A with 10 nm-well width.

which was accompanied by the increasing PL intensity of the band at 1.7 eV with decreasing temperature. Further decrease in temperature from 100 K to 10 K resulted in the decrease of the PL intensity. The reasons for this behavior should be related to the changes in PL quantum efficiency and/or the new phase transition of Alq_3 at the specific temperature[21].

Photocurrent

Fig. 6 showed PC of structure B on p-Si with different TPD thickness. PC of all indicated a wide range of response wavelengths from 1-2.7 eV or 450-1100 nm. This feature suggested an application of this structure for a wide range of photodetectors. All PC signals
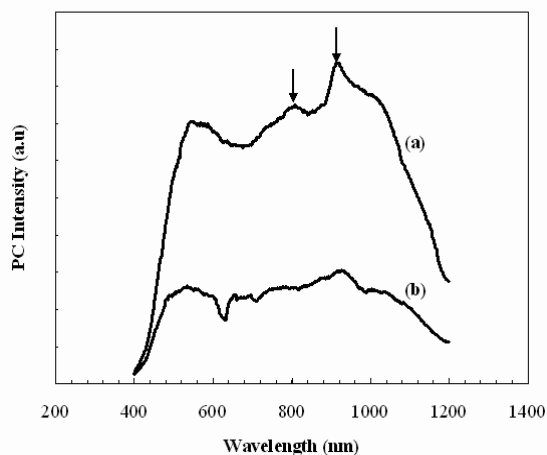
Fig 6. Photocurrent of structure B with different TPD thickness (a) 100 nm thick, (b) 5 nm thick.
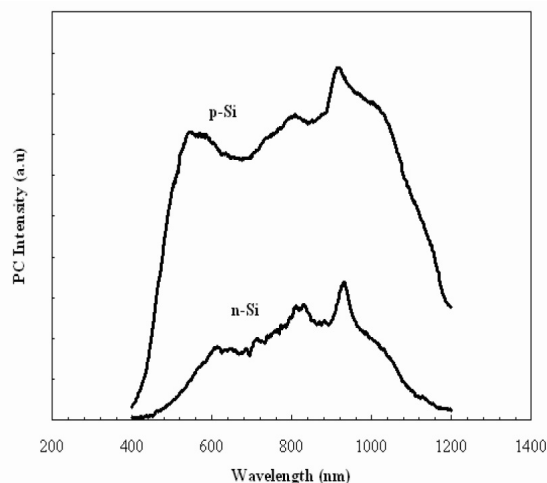
Fig 7. Photocurrent of structure B on different type of Si substrate.

decreased significantly when photon energy was above 2.7 eV because photons with photon energy greater than the energy gap of ZnSe of 2.7 eV were absorbed by the ZnSe layer and then recombined nonradiatively. The PC signals also showed two pronounced maxima at 830 and 950 nm as indicated by arrows. When the sample was illuminated, photons with energy lower than energy gap of Alq_3 and TPD could penetrate to silicon substrate at which they could be absorbed. These two peaks were, therefore, attributed to fundamental absorption of the silicon layer[23]. As the TPD thickness varied from 5 – 100 nm, the PC of the sample increased with increasing TPD thickness. The sample with 100 nm thick TPD showed the most significant improvement in the PC intensity, compared with other samples. From this behavior, it can be concluded that the TPD layer played an important role in photo-generated current process, especially in the visible range. As the TPD thickness increased, more photo-excited carriers were generated, reflecting in the increment of the PC signal. Effect of Alq_3 on the PC intensity of the sample was studied and found that the increase in the Alq_3 layer caused the decrement of the PC intensity. This effect is in contrast to the effect of TPD thickness on the PC intensity. These two features implied that the change in electron transport layer (Alq_3), and hole transport layer (TPD) can state the location of photo-induced current process. In this structure, the PC process should take place at the TPD layer. In addition, as the Alq_3 thickness increased, less number of photons could penetrate into the TPD layer, reflecting the decrease in the PC signal. We had grown structure B sample on different types of Si substrate. The PC signals of the sample are shown in Fig. 7. The PC intensity of the sample grown on p-Si was approximately three times greater in magnitude than
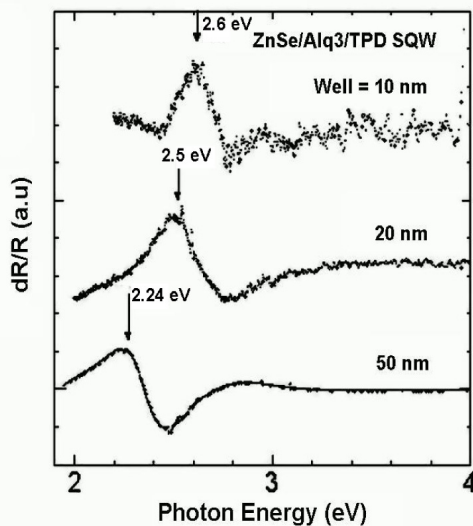
the value of the sample grown on n-Si. This behavior implied that TPD, which was the hole transport layer and was in contact with p-Si of which majority were holes, could improve the PC signal. More holes from p-Si could additionally aid the photon-generated current process, reflecting the greater current than the signal of the sample grown on n-Si whose majority carriers were electrons.

Electroreflectance

The ER spectrum of structure B with different thickness of the Alq_3 layer is shown in Fig 8. From the ER spectra, the transition energies increased with the decreasing Alq_3 thickness. The transition energies increased from 2.24 eV to 2.6 eV with the decreasing Alq_3 thickness from 50 to 10 nm. The results showed the same feature observed in a new class of superlattice materials consisting of alternating layers of Alq_3 and MgF_2 by vacuum deposition[24]. The changes of the exciton energy could be interpreted as the confinement effects of exciton in the Alq_3 thin layers. Therefore, this structure formed a single quantum well. In order to analyze such complicated behavior of the ER spectra, we carried out a line shape analysis by using the low-field ER spectrum proposed by Aspnes[26]. We have fitted the measured spectra and modulated reflectance dR/R. The ER spectra as a function of photon energy can be analyzed using Aspnes third-derivative function in the low electric field limit[25], i.e.

$$\frac{dR}{R} = \text{Re} \sum_{j=1}^{p} C_j e^{i\theta_j} (E - E_{gi} + i\Gamma_j)^{-n} \qquad (1)$$
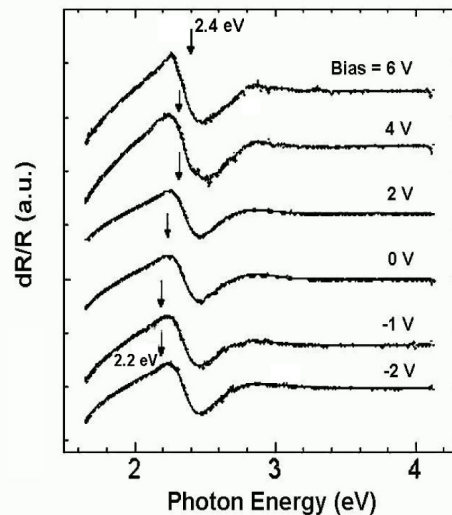
Where R is the reflectance; dR is the induced change in the reflectance by modulation light; E is the photon energy; p is the total number of spectral structures to be fitted; E_{gi}, Γ_j, C_j and θ_j are transition energy, broadening parameter, amplitude and phase, respectively, of the feature corresponding to the jth critical point. An exponent n is a characteristic parameter which depends on the type of the critical point and the order of derivative. In all cases, the spectra were fitted with $n = 3$, indicating a two-dimensional critical point. E_{gi}, Γ_j, C_j and θ_j were varied and fitted. In this experiment, only one critical point was determined. The energy level associated with transition energy was determined by least-square fitting of Eq. (1) to ER spectra obtained experimentally. In this calculation, the n value was 3 for the quantum well transition feature[26]. The transition energies determined by the fittings are indicated by arrows, as shown in Fig. 8. The transition energy decreased with the increasing quantum well width. As the quantum well width increased, the quantized energy level in the quantum well decreased, reflecting the decrease of the transition energy in the well. The properties of film with larger thickness should be similar to that of bulk which the effect of quantum confinement is small.

Fig. 9 showed the ER spectra of structure B with 50 nm Alq_3 layer measured in applied DC voltages from +6 to -2 V. The transition energies obtained from these fittings are indicated by arrows. The peaks showed a significant red shift from 2.24 eV to about 2.2 eV with increasing applied negative voltage from 0 to -2 V. With forward bias from 0 to +6 V, the ER peak exhibited a blue shift from 2.24 eV to 2.4 eV. Such red-shift and blue-shift are clearly due to the quantum confined Stark shift.

Fig 8. Room temperature-ER spectra of structure B as a function of the well thickness. The arrows indicate the transition energies determined by the fittings.

Fig 9. ER spectra of structure B with 50-nm Alq_3 layer measured in applied voltage +6.0 ~ -2.0V.

Conclusion

Inorganic/organic heterostructures of ZnSe/Alq$_3$/ZnSe and ZnSe/Alq$_3$/TPD on Si- substrate were grown by electron-beam evaporator. It was found that ZnSe/Alq$_3$/ZnSe form type-I single quantum well structure. AFM images showed that the roughness of Alq$_3$ surface increased as the thickness increased. The nanocrystal ZnSe potential barrier layer grown by the same technique was in good uniformity. PL measurement clearly showed the recombination of confined excitons in the quantum well. Temperature-dependent PL that increased with decreasing temperature, exhibited the thermal population of exciton state in the well. For other structure of ZnSe/Alq$_3$/TPD on Si substrate, the effect of thickness of TPD layer, Alq$_3$ layer, and type of Si substrate were revealed by PC. The wavelength response of the structures covered visible to near infrared spectrum. From the experiment, it could be concluded that TPD played a crucial role in PC process of this device, especially in the visible range. The effect of type of Si substrate indicated that p-Si could improve the PC intensity. The ER spectra of this structure showed the optical transition energies in quantum well as Alq$_3$ quantum well thickness was varied from 10 to 50 nm. The ER signals also showed the significant Stark shift when the device was under applied electric field.

References

1. Parker ID, Pei Q, and Marrocco M (1994) Efficient blue electroluminescence from a fluorinated polyquinoline. *Appl Phys Lett* **65**, 1272-4.
2. Burrows PE, and Forrest SR (1994) Electroluminescence from trap-limited current transport in vacuum deposited organic light emitting devices. *Appl Phys Lett* **64**, 2285-7.
3. Tang CW, and Vanslyke SA (1987) Organic electroluminescent diodes. *Appl Phys Lett* **51**, 913-5.
4. Qiu C, Chen H, Wong M, and Kwok HS (2004) Efficient blue to violet organic light-emitting diodes. *Synth Met* **140**, 101-4.
5. Lu MH, and Sturm JC, (2002) Optimization of external coupling and light emission in organic light-emitting devices: modeling and experiment. *J Appl Phys* **91**, 595-604.
6. Peumans P, Bulovic V, and Forrest SR (2000) Efficient, high-bandwidth organic multilayer photodetectors. *Appl Phys Lett* **76**, 3855-7.
7. Tang CW (1986) Two-layer organic photovoltaic cell. *Appl Phys Lett* **48**, 183-5.
8. Agranovich VM, Basko DM, La Rocca GC, and Bassani F (2001) New concept for organic LEDs: non-radiative electronic energy transfer from semiconductor quantum well to organic overlayer. *Synth Met* **116**, 349-51.
9. Agranovich VM, La Rocca GC, and Bassani F (1997) Efficient electronic energy transfer from semiconductor quantum well to an organic material. *JETP Lett* **66**, 748-51.
10. Era M, Maeda K, and Tsutsui T (1998) Self-organization approach to organic/inorganic quantum-well based on metal halide-based layer perovskite. *Thin Solid Films* **331**, 285-90.
11. Takada J, Awaji H, Koshioka M, Nakajima A, and Nevin WA (1992) Organic–inorganic multilayers: A new concept of optoelectronic material. *Appl Phys Lett* **61**, 2184-6.
12. Takada J (1995) Organic-inorganic hetero nanosystems as an approach to molecular optoelectronics. *Jpn J Appl Phys* **34**, 3864-70.
13. Qiu CF, Wang LD, Chen HY, Wong M, and Kwok HS (2001) Room-temperature ultraviolet emission from an organic light-emitting diode. *Appl Phys Lett* **79**, 2276-8.
14. An H, Hou J, Chen B, Shen J, and Liu S (1998) Fabrication and characterization of high quality organic multiple quantum well structures. *Thin Solid Films* **326**, 201-4.
15. Nukeaw J, Fujiwara Y, and Takeda Y (1997) Observation of electric fields at surface and interface of doped GaAs/semi-insulating GaAs structures by fast Fourier transformed PR. *Jpn J Appl Phys* **36**, 7019-23.
16. Nukeaw J, Fujiwara Y, Takeda Y, Funato M, Aoki S, Fujita Sz, and Fujita Sg (1998) Observation of high electric field at ZnSe/GaAs heterointerfaces by fast Fourier transformed PR. *Thin Solid Films* **334**, 11-4.
17. Hsu TM, Chang WH, Huang CC, Yeh NT and Chyi JI (2001) Quantum-confined Stark shift in ER of InAs/In$_x$Ga$_{1-x}$As self-assembled quantum dots. *Appl Phys Lett* **78**, 1760-2.
18. Kim SY, Ryu SY, Choi JM, Kang SJ, Park SP, Im S, Whang CN, and Choi DS (1998) Characterization and luminescence properties of Alq$_3$ films grown by ionized-cluster-beam deposition, neutral-cluster-beam deposition and thermal evaporation *Thin Solid Films* **398-399**, 78-81.
19. Wenge Y, Zheng X, Feng T, Shengyi Y, Lei Q, Chong Q, Shanyu Q, and Xurong X (2004) Different emission mechanism of organic-inorganic heterostructure device *Displayed* **25**, 61-5.
20. Mason MG, Tang CW, Hung LS, Raychaudhuri P, Madathil J, Giesen DJ, Yan L, Le QT et al (2001) Interfacial chemistry of Alq$_3$ and LiF with reactive metals. *J Appl Phys* **89**, 2756-65.
21. Cölle M, and Gärditz C, (2004) Delayed fluorescence and phosphorescence of tris-(8-hydroxyquinoline)aluminum(Alq$_3$) and their temperature dependence. *J Luminescence* **110**, 200-6.
22. An H, Chen B, Hou J, Shen J, and Liu S (1998) Exciton confinement in organic multiple quantum well structures. *J Phys D: Appl Phys* **31**, 1144-8.
23. Komolov A, Schumburg K, and Monakhov V (1999) Photovoltage and photoconductivity in Si/organic film/metal structures with films made of poly (3-alkylthiophene) molecules and polycyclic conjugated molecules, *Synth Met* **105**, 29-33.
24. Tokito S, Sakata J, and Taga Y (1994) Structures and optical properties of organic/inorganic superlattices. *Appl Phys Lett* **64**, 1353-5.
25. Aspnes DE (1973) Third-derivative modulation spectroscopy with low-field ER. *Surf Sci* **37**, 418-42.
26. Basmaji P, Ceschin AM, Siu LM, Hipolito O, Bernussi AA, Iikawa F, and Motisuke P (1990) MBE growth and characterization of δ-doping in GaAs and GaAs/Si. *Surf Sci* **228**, 356-8.